

Synthesis, growth and characterization of L-Alanine Potassium Chloride single crystal: a phase-matchable semi-organic material for second and third order NLO applications

S. Arockia Avila¹ · S. Selvakumar¹ · M. Francis¹ · A. Leo Rajesh¹

Received: 13 July 2016 / Accepted: 24 August 2016 / Published online: 30 August 2016
© Springer Science+Business Media New York 2016

Abstract L-Alanine Potassium Chloride single crystals have been grown by slow evaporation solution growth technique. The cell parameters were estimated from single crystal X-ray diffraction analysis and it was found that the material crystallizes in orthorhombic symmetry with space group of $P2_12_12_1$. The powder X-ray analysis proved its crystalline nature without the formation of secondary phases. The presence of functional groups and the nature of bonds appearing in the material were identified by FTIR spectroscopy. Optical constants were estimated by UV–visible spectrum and the lower cut off wavelength was observed at 330 nm. Photoluminescence emission spectrum show violet band through a strong peak centred at 380 nm. The scanning electron microscope analysis has been carried out to determine the surface morphology of the grown crystal. Energy dispersive spectrum was done to identify the composition of elements present in the title material. The second harmonic generation efficiency of the sample was confirmed and measured by Kurtz powder technique which reveals that the conversion efficiency was found to be two times that of urea crystal. Third order nonlinear optical susceptibility was identified using Z-scan technique and it is found that the crystal has a positive refractive index which is self focusing in nature. The obtained results show that L-Alanine KCl crystals are potential materials in NLO device applications.

1 Introduction

In recent years, non-linear optical (NLO) crystals with high conversion efficiencies are needed for optical second harmonic generation (SHG) because of their applications in opto-electronics, photonics, high speed information processing, telecommunications and optical information storage devices [1]. Amino acid family crystals are promising materials for these applications and it depends on the properties such as transparency, birefringence, refractive index, dielectric constant and thermal, photochemical and chemical stability [2]. Amino acids are considered to be interesting organic materials for NLO devices as they contain donor carboxylic (COOH) group and the proton acceptor amino acid (NH₂) group known as zwitterions which create hydrogen bonds. Considerable efforts have been made on amino acid mixed complex crystals in order to make them suitable for device fabrications [3–6]. L-Alanine is an efficient organic NLO material under the amino acid category. The structural arrangement of LAL (head to tail bond sequence) and the occurrence of π - π^* transition in the carboxylic group, accounts for its nonlinearity having the SHG efficiency as one third of the well-known KDP [7]. Several new complexes of L-Alanine with improved NLO properties have been reported [8–13].

Most of the organic NLO crystals usually have poor mechanical and thermal properties and the inorganic NLO materials have excellent mechanical and thermal properties, but possess relatively modest optical nonlinearity therefore semiorganic crystals are those which combine the positive aspects of organic and inorganic materials resulting in desired nonlinear optical properties [14]. The properties of large nonlinearity, high resistance, low angular sensitivity, good mechanical hardness and the further significance are centred on semi organic crystals. Hence,

✉ A. Leo Rajesh
aleorajesh@gmail.com

¹ Department of Physics, St. Joseph's College,
Tiruchirappalli 620 002, India

investigations were done to develop various semiorganic crystals which are more suitable for device fabrication by Selvakumar et al., [15–19]. Photo induced effects in L-Alanine crystals were studied by A.Wojciechowski et al. [20] in which the optical absorption and SHG were analysed post photo treatment by different laser devices during different time periods.

The present manuscript reports on the crystal growth of L-Alanine KCl crystals from aqueous solution followed by the characterizations like single crystal X-ray diffraction, powder X-ray diffraction, Fourier transform infrared spectroscopy, UV–Vis–NIR spectroscopy, scanning electron microscopy, elemental analysis, second harmonic generation efficiency and Z-scan studies. Estimation of optical constants, third order NLO susceptibility and particle size dependency analysis are the highlights of the present work.

2 Experimental

2.1 Materials and method

The precursor materials used in the present work were of analytical reagent (AR) and guaranteed reagent (GR) grade. L-Alanine (Loba, 98 % GR) and Potassium Chloride (Merck, 99 % AR) were used as precursors. Double deionized water (Merck) was used as a solvent. Slow evaporation solution growth technique was adopted for the growth of single crystals [21]. The entire reaction was carried out at room temperature. L-Alanine and Potassium Chloride were taken in equimolar ratio and stirred well for 4 h separately. The solution was then filtered and kept in a vibration free ambiance. Transparent seed crystals were obtained by spontaneous nucleation. Among them, defect free seed crystal was suspended in the mother solution. Optically good quality crystals of dimension $10 \times 5 \times 8 \text{ mm}^3$ have been grown within the period of 25 days. The photograph of the grown crystal was shown in Fig. 1.

2.2 Characterization techniques

The grown crystals were subjected to various characterization analyses to test their suitability for optical device applications. Single crystal X-ray diffraction analysis was carried out using Four-circle Enraf–Nonius CAD4/MACH3 single crystal diffractometer to determine the lattice parameters and space group. Powder X-ray diffraction studies were carried out using XPERT-PRO X-ray diffractometer with $\text{CuK}\alpha$ ($\lambda = 1.5418 \text{ \AA}$) radiation. The presence of functional groups in the grown crystal was identified using Fourier transform infrared spectral analysis using a PERKIN ELMER SPECTROMETER by KBr

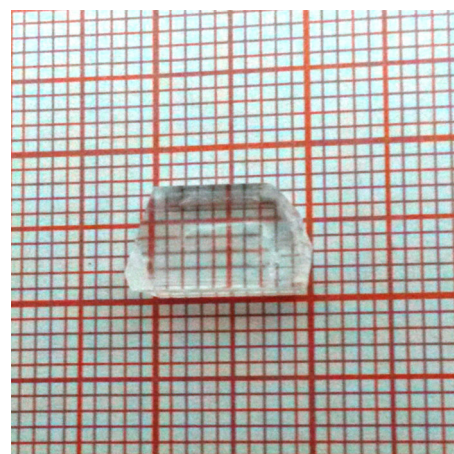


Fig. 1 As grown L-Alanine KCl single crystal

pellet technique. In order to examine the optical properties of the grown crystal in the UV–Vis–NIR regions of electromagnetic spectrum, the linear optical study was carried out using PERKIN ELMER LAMBDA 35 UV–visible spectrophotometer. SEM analysis was carried out by using JEOL 6360 TESCAN scanning electron microscope equipped with EDAX to analyse the crystal surface morphology and the elements present in the L-Alanine KCl crystal. Second Harmonic Generation efficiency test for the grown samples was performed by Kurtz and Perry powder technique using a Q-switched high energy Nd:YAG Laser (QUANTA RAY Model LAB-170-10) Model HG-4B-High efficiency with repetition rate at 10 Hz. Photoluminescence spectrum was recorded using CARY ECLIPSE with a scan rate of 600 nm/min. Third order nonlinear optical susceptibility was identified using a He–Ne laser of wavelength 632.8 nm.

3 Results and discussion

3.1 Single crystal XRD analysis

The L-Alanine KCl crystal was subjected to single crystal X-ray diffraction analysis to determine the lattice parameters and space group. The title compound crystallizes into orthorhombic system with non-centrosymmetric space group $P2_12_12_1$. From the XRD data, the calculated lattice parameter values are found to be $a = 5.782 \text{ \AA}$, $b = 6.015 \text{ \AA}$, $c = 12.312 \text{ \AA}$, $\alpha = \beta = \gamma = 90^\circ$ and cell volume $V = 428.3 \text{ \AA}^3$ and are tabulated in Table 1.

3.2 Powder X-ray diffraction analysis

The crystallinity and phase of the grown crystal was studied by powder X-ray diffraction. The crystalline nature

Table 1 Single crystal XRD analysis data of L-Alanine KCl

| L-Alanine KCl | Crystal data |
|----------------------|---|
| Crystal system | Orthorhombic |
| Space group | P2 ₁ 2 ₁ 2 ₁ |
| Unit cell dimensions | a = 5.782 Å b = 6.015 Å c = 12.312 Å α = β = γ = 90° |
| Volume | 428.3 Å ³ |
| C/a ratio | 1.0402 |
| FWHM | 0.1476 |

of the synthesized material is well revealed by the prominent peak at specific 2θ angle. The powder XRD pattern of L-Alanine KCl is shown in Fig. 2. The changes in lattice parameters are responsible for the shifting of prominent peaks and in addition to that small variations in the intensities are also observed.

3.2.1 Calculation of crystallite size, micro strain and bond length

The average crystallite size of the samples is calculated using Debye–Scherrer formula

$$D = \frac{0.9\lambda}{\beta \cos \theta}$$

where, λ is the wavelength of the radiation used; β is the full width half maximum; θ is the angle of diffraction

Micro strain (ε) is calculated using the expression

$$\epsilon = \frac{\beta \cos \theta}{4}$$

The bond length of the L-Alanine KCl crystal is given by

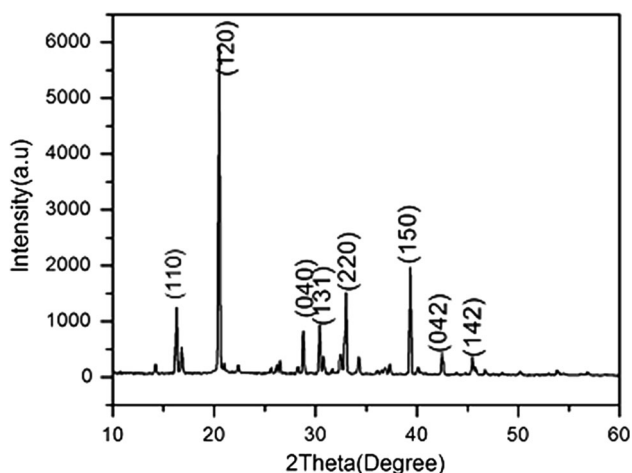


Fig. 2 Powder XRD pattern of L-Alanine KCl

$$l = \sqrt{\frac{a^2}{3} + \left(\frac{1}{2} - u\right)^2 c^2}$$

$$u = \frac{a^2}{3c^2} + 0.25$$

The lattice parameters of the sample are calculated by the method of least squares.

$$\lambda = 2d_{hkl} \sin \theta_{hkl}$$

$$\frac{1}{d^2} = \left(\frac{h^2}{a^2}\right) + \left(\frac{k^2}{b^2}\right) + \left(\frac{l^2}{c^2}\right)$$

$$V = abc$$

where d is the lattice spacing, hkl is the miller indices, abc is the lattice parameters, λ is the wavelength of the X-rays, V is the volume of the unit cell, and 2θ is the diffraction angle.

The lattice parameters a and c are given by the equation

$$a = \frac{\lambda}{\sqrt{3}} \sin \theta$$

$$c = \frac{\lambda}{\sin \theta}$$

The theoretical lattice parameters and the experimental lattice parameters obtained from powder XRD and single crystal XRD analysis are presented in Table 2. It is evident from the table that the material has retained its orthorhombic structure.

3.3 Fourier transform infrared spectral analysis

Fourier transform infrared spectral studies were carried out for the samples to identify the functional groups. The presence of functional groups in the compound L-Alanine and Potassium Chloride was identified and is shown in Fig. 3. The vibration peak at 3097 cm⁻¹ with medium intensity represents C–H asymmetric stretching. The absorption peak at 2592 cm⁻¹ with weak intensity shows OH stretching. The absorption band at 1628 cm⁻¹ with strong intensity represents C=O stretching. The sharp peak at 1353 cm⁻¹ with medium intensity represents C–H in plane bending. The absorption peak at 1016 cm⁻¹

Table 2 Experimental lattice parameter values obtained from powder XRD and single crystal XRD analysis of L-Alanine KCl

| | |
|------------------------|-------------|
| Crystallite size (D) | 16.25 nm |
| Micro-strain (ε) | 2.0815002 |
| Bond length (l) | 3.661210236 |
| Lattice parameters (a) | 6.076 |
| Lattice parameters (c) | 5.2262 |
| C/a ratio | 0.86013 |

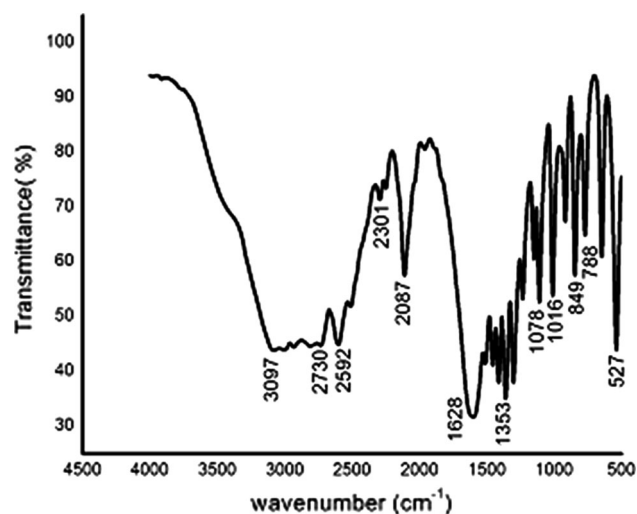


Fig. 3 FTIR spectrum of L-Alanine KCl

represents C–CHO stretching. The vibration peak at 849 cm^{-1} strong band refers to C–H out of plane bending. The absorption band at 788 cm^{-1} with strong band refers C–H out of plane bending. The strong absorption peak at 527 cm^{-1} band refers to O–CN deformation. The vibrational frequencies of various functional groups of L-Alanine KCl are presented in Table 3.

3.4 UV–visible NIR spectral analysis

Optical transparency in the entire visible region with a good percentage of transmission is the key properties of an NLO material. Figure 4 shows the UV–visible–NIR transmission spectrum of L-Alanine KCl. {Inset shows Refractive index vs Wavelength of L-Alanine KCl and Plot of optical conductivity vs $h\nu$ of L-Alanine KCl}. From the figure it is observed that the material has high transmittance in the entire visible region of about 65 % without any strong absorption in the visible region and the lower cut off wavelength is observed at 310 nm. This is one of the most

Table 3 Tentative assignments of L-Alanine KCl

| Wavenumber (cm^{-1}) | Assignment |
|---------------------------------|----------------------------|
| 3097 | C–H assymmetric stretching |
| 2592 | OH stretching |
| 1628 | C=O stretching |
| 1353 | C–H bending (in plane) |
| 1016 | C–CHO stretching |
| 849 | C–H out of plane bending |
| 788 | C–H out of plane bending |
| 527 | OCN deformation |

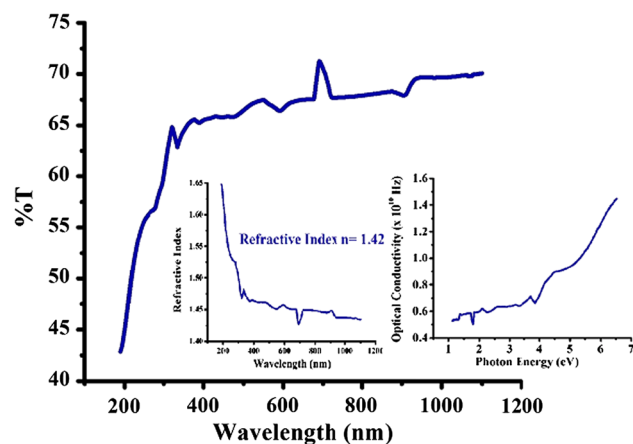


Fig. 4 UV–visible–NIR transmission spectrum of L-Alanine KCl. {Inset shows refractive index vs wavelength of L-Alanine KCl and Plot of optical conductivity vs $h\nu$ of L-Alanine KCl}

desirable properties of the NLO material for device fabrication.

3.4.1 Calculation of optical constants

Optical constants such as the optical band gap, extinction coefficient and refractive index of L-Alanine KCl crystals are estimated from the following relations. The optical band gap (E_g) of L-Alanine-KCl crystals was estimated from the relation

$$h\alpha\nu = A(h\nu - E_g)^{1/2}$$

where A is the constant, h is the planck's constant, ν is the frequency of the incident photons, α is the extinction coefficient which can be obtained from the transmittance value

$$\alpha = \frac{2.3026 \log\left(\frac{1}{T}\right)}{t}$$

Extinction coefficient (K) can be obtained from the relation

$$K = \frac{\alpha\lambda}{4\pi}$$

The reflectance (R) and refractive index (n) were derived from the relations

$$R = \frac{1 \pm \sqrt{(1 - \exp(-\alpha t) + \exp(\alpha t))}}{(1 + \exp(-\alpha t))}$$

$$n = \frac{-(R + 1) \pm \sqrt{(-3R^2 + 10R - 3)}}{2(R - 1)}$$

The refractive index was calculated from the plot of wavelength versus refractive index and it was found to be $n = 1.42$.

3.5 Morphological studies

Scanning electron microscopy (SEM) analysis has been carried out for the grown crystal to study the nature, surface morphology and the presence of imperfections in the grown crystals. The transparent regions of the crystals are cut into few mm for examining the surface morphology. From the SEM micrograph it is clearly seen that the surface of the grown crystal appears to be very smooth and is shown in Fig. 5. The micro particles are attached with one another forming a disordered heap pattern. Influenced by the crystal growth conditions and the presence of certain inclusions formed during the crystal growth, the surface appears to be smooth even though after the addition of Potassium Chloride.

During the synthesis process at low temperature weakly attached impurities and vacancies are present in the crystal lattice. At high temperature the attached water molecule is lost and a fracture is developed causing intrinsic defects. Hence L-Alanine ions occupy some interstitial positions, creating defects due to which the particles are closely packed. This is clearly observed from SEM analysis.

Energy dispersive X-ray analysis (EDX) is a micro-analytical technique which is used to obtain information regarding the chemical composition of the grown crystal. A fine beam of X-rays is made to fall into the sample. The energy of the X-rays emitted by the sample is measured by an energy-dispersive spectrometer. Since the energy of the X-rays emitted from the sample is attributed to the energy difference between the two shells and of the atomic structure of the compound, the elemental composition of the specimen can be measured and the percentage of

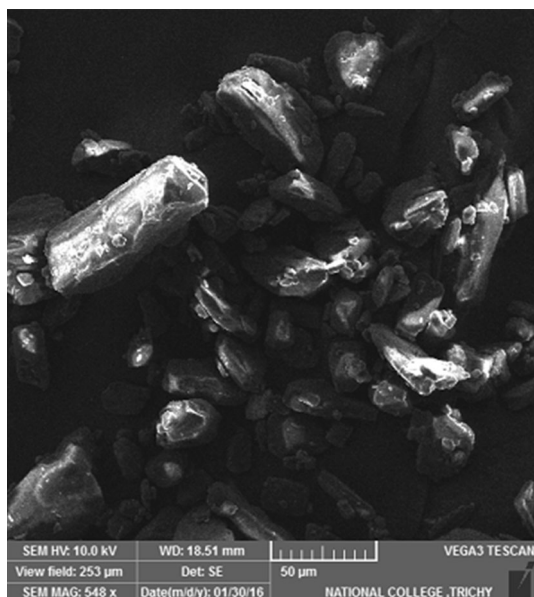


Fig. 5 Magnification of SEM micrograph of L-Alanine KCl

inclusions in the sample are presented in Table 4. From the EDX analysis, the presence of Potassium Chloride in the grown specimen is confirmed and is shown in Fig. 6.

3.6 Photoluminescence study

Photoluminescence emission spectrum was recorded within the wavelength range of 300–475 nm and is shown in Fig. 7. The sample was excited at 361 nm and the emission peak is observed around 382 nm which corresponds to violet radiation. The sharp intensified peak around 382 nm is assigned to $n-\pi^*$ transition of carbonyl group. The PL intensity decreases with increase in wavelength. This is attributed to the rotation of carbonyl group around the C–C bond. The important feature of optical transitions in organic materials is the energy difference between the absorption and emission peaks which is known as Stoke's shift. This shift is the measure of interfacial fluctuations which varies with position. Carriers are photo excited uniformly, but they diffuse to regions where the confinement energy is smaller before recombination. Hence this causes the intensity of the emission peak to be less than that of the excitation peak.

3.7 Second harmonic generation test

Second Harmonic Generation efficiency of L-Alanine KCl crystal was determined by Kurtz and Perry technique. Finely powdered samples are packed tightly in a micro capillary tube. The SHG efficiency of the L-Alanine KCl material is measured with respect to the efficiency of the urea crystals. A photomultiplier tube is used to detect the frequency conversion process which results in the emission of green emission. A Q-switched Nd:YAG laser emitting fundamental wavelength of 1064 nm is allowed to strike on the powdered sample. The experiment is carried out at room temperature [22]. The input energy used is 3.2 mJ/pulse with a pulse width of 8 ns. SHG efficiency measurement is an initial screening method to observe the phase matching behaviour of a material. In order to confirm the existence of phase matching property, the intensity dependence on particle size of L-alanine KCl powder sample is studied. The SHG intensity increases almost

Table 4 EDAX quantification table of L-Alanine KCl

| Element | Weight% | Atomic% |
|-----------|---------|---------|
| Carbon | 65.32 | 72.01 |
| Oxygen | 33.17 | 27.45 |
| Chlorine | 0.81 | 0.30 |
| Potassium | 0.70 | 0.24 |
| Totals | 100.00 | 100.00 |

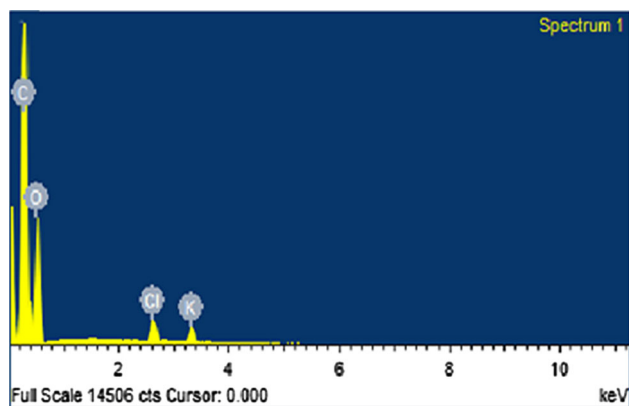


Fig. 6 EDAX spectrum of L-Alanine KCl

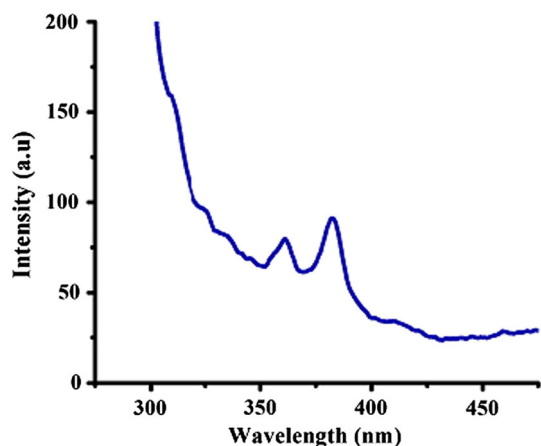


Fig. 7 PL emission spectrum of L-Alanine KCl

linearly with the increase in the particle size until 355–500 μm and above this range, it deviates from the linearity and starts to attain saturation. This kind of particle size dependency of SHG intensity is also observed in phase matchable crystals [23] and the particle size dependency of the title material is shown in Fig. 8. Only the crystals exhibiting phase matching activity are grown into high pure defect free bulk single crystal for NLO devices. The particle size dependency of SHG intensity is studied to affirm the phase matching nature of the materials. SHG efficiency of a particle strongly depends on the particle size.

The estimated output energies of Urea and L-Alanine KCl crystal are 8.9 mJ and 18 mJ respectively. The SHG efficiency of L-Alanine KCl crystal is observed to be two times that of urea crystal and it confirms the suitability of L-Alanine KCl crystals in NLO applications. The powdered crystals are sieved accordingly into different sizes using Haver EML sieve shaker. Urea crystal is used as a reference material. Hence urea crystal is also grinded and sieved to the ranges of same particle size. A linear increase of the SHG intensity is observed in the particle size. The linearity

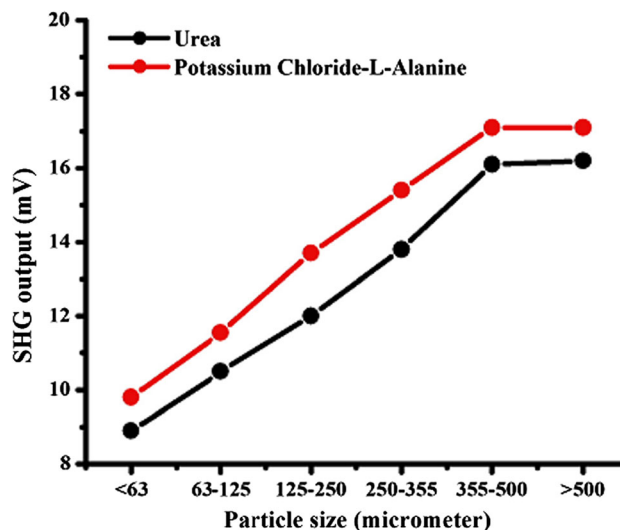


Fig. 8 Particle size dependency of L-Alanine KCl

of the curve is maintained till and this indicates the phase matching nature of the particles. Hence L-Alanine KCl crystals are best suited for frequency conversion applications.

3.8 Z-scan technique

Z-scan technique was originally introduced by Sheik Bahae et al. [24, 25]. This is a simple and sensitive single beam technique to measure the sign and magnitude of both real and imaginary part of third order nonlinear susceptibility, $\chi^{(3)}$. In the original single beam configuration, the transmittance of the sample is measured, as the sample is moved, along the propagation direction of a focussed Gaussian laser beam. A laser beam propagating through a nonlinear medium will experience both amplitude and phase variations. If transmitted light is measured through an aperture placed in the far field with respect to focal region, the technique is called closed aperture Z-scan experiment. In this case, the transmitted light is sensitive to both nonlinear absorption and nonlinear refraction. In a closed aperture Z-scan experiment, phase distortion suffered by the beam while propagating through the nonlinear medium is converted into corresponding amplitude variations. On the other hand, if transmitted light is measured without an aperture (in this case the entire light is collected), the mode of measurement is referred to as open aperture Z-scan. In this case, the throughput is sensitive only to the nonlinear absorption. Closed and open aperture Z-scan graphs are always normalized to linear transmittance i.e. transmittance at large values of $|z|$. Closed aperture Z-scan and open aperture Z-scan experiments respectively yield the real and imaginary parts $\chi^{(3)}$. Usually closed aperture Z-scan data is divided by open aperture

data both measured simultaneously, to cancel the effect of nonlinear absorption contained in the closed aperture measurement. The new graph, called divided Z-scan graph, contains information on nonlinear refraction alone. In a Z-scan measurement, it is assumed that sample is thin, i.e. the sample length is much less than Rayleigh’s range Z_o . [$Z_o = k\omega_o^2/2$ where k is the wave vector and ω_o is the beam waist]. This is essential to ensure that beam profile does not vary appreciably inside the sample. Photodetector (PDI) monitors the input laser energy. PD2 and PD3 give open and closed aperture measurements respectively. Different variants of this technique such as eclipsing Z-scan and two colour Z-scan have also been introduced [26–28].

In non degenerate (two colour) Z-scan, the effect of nonlinear refraction and absorption induced by a strong excitation beam at a frequency ω_e on a weak probe beam at a different frequency ω_p i.e. $\Delta n(\omega_e, \omega_p)$ and $\Delta\alpha(\omega_e, \omega_p)$ are measured. [Δn refers to the change in refractive index and $\Delta\alpha$ refers to the change in absorption coefficient]. Non degenerate Z-scan technique has some advantages over conventional single beam technique. The frequency difference $(\omega_p - \omega_e)$ can be exploited to get information about the dynamics of the nonlinear response with time resolution much less than the laser pulse width. With two colour Z-scan technique, it is possible to make time resolved measurements by suitably delaying the probe pulse with respect to pump beam. Investigation of non-degenerate nonlinearity has technological importance in the area of dual wavelength all optical switching applications, where cross phase modulation is very important. In eclipsing Z-scan technique, the far field aperture is replaced with an obscuration disk, which blocks most of the beam. This modification of the Z-scan technique enhances sensitivity to induced wave front distortion to an order of $\lambda/10^4$. Two colour eclipsing Z-scan technique has also been suggested [29].

The third order nonlinear refractive index n_2 and the nonlinear absorption coefficient β of L-Alanine KCl crystal are evaluated by the measurements of Z-Scan. The technique is performed using a He–Ne laser of wavelength 632.8 nm. The sample was translated in the z-direction along the axis of the focussed Gaussian beam from He–Ne laser source, and the variation in the far field intensity of the beam from the laser source with the sample position is measured. The amplitude of the phase shift is determined thoroughly by monitoring the change in the resistance through a small aperture at the far field position (closed aperture). Intensity dependent absorption of the sample is measured by moving the sample through the focus and without placing the aperture at the detector (open aperture) Fig. 9a, b. By focusing a beam of laser through the crystal, a spatial distribution of the temperature in the crystal surface is produced. Hence a spatial variation in refractive

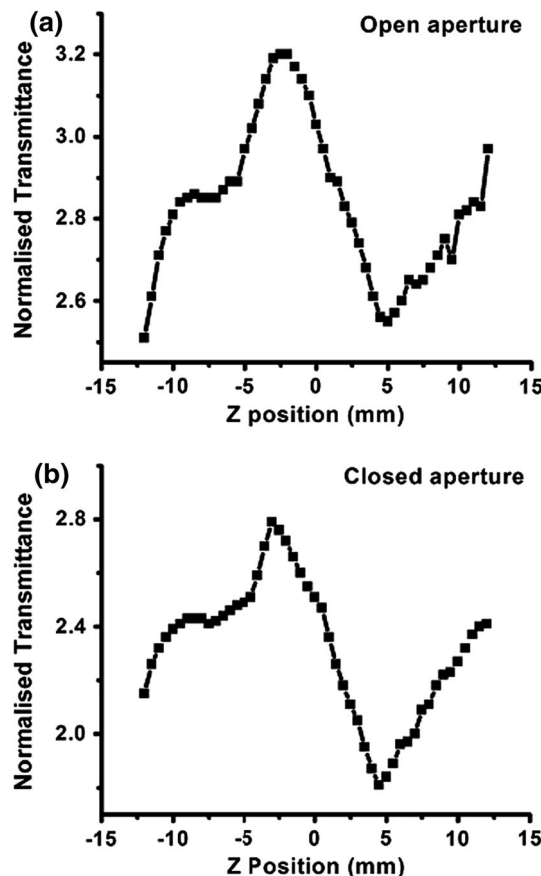


Fig. 9 a Z Scan open aperture of L-Alanine KCl. b Z Scan closed aperture of L-Alanine KCl

index is created, which acts as a thermal lens, resulting in the phase distortion of the propagating beam.

The difference between the peak and the valley transmission (ΔT_{P-V}) is given in terms of the on-axis phase shift at the focus as,

$$\Delta T_{P-V} = 0.406(1 - S)^{0.25} |\Delta\Phi|$$

where S is the aperture linear transmittance and is calculated by using the relation $S = 1 - \exp\left(\frac{-2r_a^2}{w_a^2}\right)$ where r_a is the aperture radius and w_a is the beam radius at the aperture. The nonlinear refractive index (n_2) is given by the expression [30, 31],

$$n_2 = \frac{\Delta\Phi}{KI_oL_{eff}}$$

where $K = \frac{2\pi}{\lambda}$ in which, λ is the wavelength of the laser light, I_o is the intensity of the laser beam at the focus ($Z = 0$), L_{eff} is the effective thickness of the crystal, L is the thickness of the crystal which is calculated using the expression,

Table 5 Measurement details and the results of the Z-scan technique

| | |
|--|--|
| Laser beam wavelength (λ) | 632.8 nm |
| Lens focal length (f) | 8.5 cm |
| Optical path distance (Z) | 115 cm |
| Spot-size diameter in front of the aperture (ω_a) | 1 cm |
| Aperture radius (r_a) | 4 mm |
| Incident intensity at the focus (Z = 0) | 20 $\mu\text{W}/\text{cm}^2$ |
| Effective thickness (L_{eff}) | 0.9980 mm |
| Linear absorption coefficient (α) | 2 |
| Nonlinear refractive index (n_2) | $3.500 \times 10^{-1} \text{ cm}^2/\text{W}$ |
| Nonlinear absorption coefficient (β) | $2.636 \times 10^5 \text{ cm}/\text{W}$ |
| Real part of the third-order susceptibility | $5.6680 \times 10^{-3} \text{ esu}$ |
| Imaginary part of the third-order susceptibility | $2.261 \times 10^{-4} \text{ esu}$ |

$$L_{\text{eff}} = \frac{1 - e^{-\alpha L}}{\alpha}$$

From the open aperture Z-scan data, the nonlinear absorption coefficient (β) is determined by using the relation,

$$\beta = \frac{2\sqrt{\Delta T}}{I_0 L_{\text{eff}}}$$

where ΔT is the one valley value at the open aperture Z-scan curve. From the n_2 and β values the real and imaginary part of the third order nonlinear optical susceptibility are determined. These are obtained by using the relations,

$$\text{Re } \chi^{(3)}(\text{esu}) = 10^{-4} (\epsilon_0 C^2 n_o^2 n_2) / \pi \text{ in cm}^2/\text{W}$$

$$\text{Im } \chi^{(3)}(\text{esu}) = 10^{-2} (\epsilon_0 C^2 n_o^2 \lambda \beta) / (4\pi^2) \text{ in cm}^2/\text{W}$$

where ϵ_0 is the permittivity of free space, n_o is the linear refractive index of the crystal, and C is the velocity of light in vacuum.

$$|\chi^{(3)}| = \left[(\text{Re}(\chi^{(3)}))^2 + (\text{Im}(\chi^{(3)}))^2 \right]^{1/2}$$

The third order nonlinear refractive index and the nonlinear absorption coefficient are evaluated from the Z-scan measurements. Table 5 shows the experimental details and the results of Z-scan technique for L-Alanine KCl. The calculated value of nonlinear refractive index (n_2) is $3.500 \times 10^{-1} \text{ cm}^2/\text{W}$. The crystal has a positive refractive index (i.e. self focusing) [32, 33]. The self focusing nature of the sample is due to the thermal nonlinearity resulting from the absorption of radiation at 632.8 nm. From the open aperture Z-scan curve, the nonlinear absorption coefficient (β) is found to be $2.636 \times 10^5 \text{ cm}/\text{W}$. This concludes that the nonlinear absorption coefficient is

regarded as two-photon absorption [34, 35]. The real and imaginary part of the third order susceptibility ($\chi^{(3)}$) is found to be 5.6680×10^{-3} and $2.261 \times 10^{-4} \text{ esu}$.

4 Conclusion

A semiorganic NLO material L-Alanine KCl was grown by slow evaporation solution growth technique. The harvested crystals of size $10 \times 5 \times 8 \text{ mm}^3$ were obtained after a period of 25 days. Unit cell parameters were evaluated by single crystal X-ray diffraction analysis, which confirmed that the grown crystal belongs to orthorhombic system with space group $P2_12_12_1$. Powder X-ray diffraction analysis confirmed that the synthesized material was highly crystalline and it was also observed that the material retained its orthorhombic structure. The various functional groups and their vibrational interactions of the grown crystal were confirmed by Fourier transform infrared analysis. The optical study shows that the crystal has high transmittance in the entire visible region of about 65 % and the lower cut off wavelength was observed at 310 nm. The crystal surface analysis shows that the surface of the grown crystal appears to be very smooth and the percentage of elements of the grown crystal was confirmed by elemental analysis. Photoluminescence emission spectrum reveals that the emission peak is observed around 382 nm which corresponds to violet radiation. The estimated SHG efficiency of L-Alanine KCl crystal was found to be two times that of urea crystal. The nonlinear absorption was regarded as a two photon absorption process due to self-focusing nature of the L-Alanine KCl crystal. Thus L-Alanine KCl crystal can be exploited as a potential material for photonics, electro-optic and SHG device applications.

References

1. U. Karunanithi, S. Arulmozhi, J. Madhavan, J. Appl. Phys. **1**, 19 (2012)
2. K.J. Arun, S. Jayalekshmi, J. Miner. Mater. Character. Eng. **8**, 635 (2009)
3. M. Lydia Caroline, M. Prakash, D. Geetha, S. Vasudevan, Spectrochim. Acta Part A **79**, 1936 (2011)
4. D. Rajan Babu, D. Jayaraman, R. Mohan Kumar, G. Ravi, R. Jayavel, J. Cryst. Growth **250**, 157 (2003)
5. G. Bhagavannarayana, B. Riscob, M. Shakir, Mater. Chem. Phys. **126**, 20 (2011)
6. S. Natarajan, G.P. Chitra, S.A. Martin, B. Dhas, S. Athimoolam, Cryst. Res. Technol. **43**, 713 (2008)
7. L. Misoguti, A.T. Varela, F.D. Nunes, V.S. Bagnato, F.E.A. Melo, J. Mendes Filho, S.C. Zilio, Opt. Mater. **6**, 147 (1996)
8. D. Rajan Babu, D. Jayaraman, R. Mohan Kumar, R. Jayavel, J. Cryst. Growth **245**, 121 (2002)
9. R. Mohan Kumar, D. Rajan Babu, D. Jayaraman, R. Jayavel, K. Kitamura, J. Cryst. Growth **275**, 1935 (2005)
10. S.K. Kushwaha, S.P. Rathee, K.K. Maurya, G. Bhagavannarayana, J. Cryst. Growth **328**, 81 (2011)
11. S. Dhanuskodi, K. Vasantha, Cryst. Res. Technol. **39**, 259 (2004)
12. N. Singh, B.K. Singh, N. Sinha, B. Kumar, J. Cryst. Growth **310**, 4487 (2008)
13. G.G. Muley, M.N. Rode, B.H. Pawar, Acta Phys. Pol. A **116**, 1033 (2009)
14. S. Natarajan, G. Shanmugam, S.A. Martin, B. Dhas, Cryst. Res. Technol. **5**, 561 (2008)
15. S. Selvakumar, S. Arockia Avila, M. Francis, V. Sathe, A. Leo Rajesh, IRJET **02**, 412 (2015)
16. S. Selvakumar, A. Leo Rajesh, J. Chem. Pharm. Sci. **11**, 89 (2015)
17. S. Selvakumar, A. Leo Rajesh, Opt. Int. J. Light Electron Opt. **127**, 6982 (2016)
18. S. Selvakumar, A. Leo Rajesh, J. Mol. Struct. **1125**, 1 (2016)
19. S. Arockia Avila, A. Leo Rajesh, J. Chem. Pharm. Sci. **9**, 129 (2016)
20. A. Wojciechowski, K. Ozga, A.H. Reshak, R. Miedzinski, I.V. Kityk, J. Berdowski, Z. Tylczynski, J. Mater. Lett. **64**, 1957 (2010)
21. D. Prabha, S. Palaniswamy, Rasayan J. Chem. **3**, 517 (2010)
22. S.K. Kurtz, T.T. Perry, J. Appl. Phys. **39**, 3798 (1968)
23. H.J. Ravindra, M.R.S. Kumar, C. Rai, S.M. Dharmaprakash, J. Cryst. Growth **294**, 318 (2006)
24. M.S. Bahae, A.A. Said, E.W. Van Stryland, Opt. Lett. **14**, 955 (1989)
25. M.S. Bahae, A.A. Said, T.H. Wei, D.J. Hagan, E.W.V. Stryland, IEEE J. Quantum Electron. **26**, 760 (1990)
26. T. Xia, D.J. Hagan, M.S. Bahae, E.W. Van Stryland, Opt. Lett. **19**, 317 (1994)
27. M.S. Bahae, J. Wang, R. De Salvo, D.J. Hagan, E.W. Van Stryland, Opt. Lett. **17**, 258 (1992)
28. H. Ma, C.B. de Araujo, Appl. Phys. Lett. **66**, 1581 (1995)
29. A. Marcano, F.E. Hernandez, A.D. Sena, J. Opt. Soc. Am. B **14**, 3363 (1997)
30. S. Venugopal Rao, N.K.M. Naga Srinivas, D. Narayana Rao, L. Giribabu, G. Bhaskar, G. Maiya, R. Philip, G. Ravindrakumar, Opt. Commun. **182**, 255 (2000)
31. P.V. Dhanaraj, N.P. Rajesh, G. Vinitha, G. Bhagavannarayana, Mater. Res. Bull. **46**, 726 (2011)
32. E.W. Vanstryland, M. Sheik-Bahae, in *Characterisation Techniques and Tabulation for Organic Nonlinear Materials*, ed. by M.G. Kuzyk, C.W. Dirk (Marcel Dekker Inc., New York, 1998), pp. 655–692
33. P. Srinivasan, M. Gunasekaran, T. Kanagasekaran, R. Gopalakrishnan, P. Ramasamy, J. Cryst. Growth **289**, 639 (2006)
34. T. Kanagasekaran, P. Mythili, P. Srinivasan, A.Y. Nooraldeen, P.K. Palanisamy, R. Gopalakrishnan, Cryst. Growth Des. **8**, 2335 (2008)
35. S. Selvakumar, A. Leo Rajesh, J. Mater. Sci. Mater. Electron. **27**, 7509 (2016)